ORIGINAL SAND 95-0350C

AMBIENT - PRESSURE SILICA AEROGEL FILMS

Conf-941144--87

SAI S. PRAKASH[a], C. JEFFREY BRINKER[a,b] AND ALAN J. HURD[c]
[a]University of New Mexico/ Sandia National Laboratories Advanced Materials Laboratory, Albuquerque, NM 87106 (USA); [b]Ceramic Synthesis and Inorganic Chemistry Department 1846, Sandia National Laboratories, Albuquerque, NM 87185 (USA); [c]Ceramic Processing Science Department 1841, Sandia National Laboratories, Albuquerque, NM 87185 (USA).

ABSTRACT

Very highly porous (aerogel) silica films with refractive index in the range 1.006-1.05 (equivalent porosity 98.5-88%) were prepared by an ambient-pressure process[1,2]. It was shown earlier using *in situ* ellipsometric imaging[1] that the high porosity of these films was mainly attributable to the dilation or "springback" of the film during the final stage of drying. This finding was irrefutably reconfirmed by visually observing a "springback" of >500% using environmental scanning electron microscopy (ESEM). Ellipsometry and ESEM also established the near cent per cent reversibility of aerogel film deformation during solvent intake and drying. Film thickness profile measurements (near the drying line) for the aerogel, xerogel and pure solvent cases are presented from imaging ellipsometry. The thickness of these films (crack-free) were controlled in the range 0.1-3.5 μm independent of refractive index.

INTRODUCTION

The extraordinary properties of aerogels including high surface areas (often > 1000 m^2/g), low refractive indices (< 1.1), low dielectric constants (< 1.7), low thermal loss coefficients (< 0.5 $W/(m^2K)$) and low sound velocities (< 100 m/s) lead to potential thin film applications such as: ultra-low dielectric constant interlayer dielectrics, reflective and anti-reflective coatings, flat panel displays, sensors, superinsulated architectural glazing and acoustic impedance matching. To date, however, the potential of aerogels in thin film applications has not been realized mainly because conventional supercritical aerogel processing is very energy intensive, often dangerous, and most importantly - not easily adaptable to continuous thin film forming operations such as dip-coating.* The ambient-pressure route overcomes these problems, enabling the preparation of thin film specimens in a continuous process, previously impossible to do within the constraints of an autoclave.

As early as in 1931, Kistler demonstrated the preparation of aerogels by the *supercritical extraction* of the pore fluid[4]. Under supercritical conditions, the drying stress (P_C) exerted by the liquid on the gel network is essentially zero (since liquid-vapor interfaces are eliminated), often causing little or no shrinkage during drying[5]. In 1992, Deshpande et al. used an alternate route to prepare bulk aerogels at *ambient pressure*[6]. In the ambient pressure process, the drying stress is finite ($|P_C| = \frac{2\gamma_{LV}\cos\theta}{r_P} > 0$, where γ_{LV} is the surface tension, θ is the contact angle and r_P is the pore radius)[7], but, due to organic modification of the gel surface, drying-related shrinkage is at least partially reversible.

* conventional aerogel films were prepared in a batch process by Hrubesh and Poco[3].

DISCLAIMER

Our previous work[1,2] described the optimized preparation of aerogel films by the ambient-pressure route and their extensive characterization using conventional and *in situ* imaging ellipsometry, FTIR and ^{29}Si NMR spectroscopy, surface acoustic wave-based gas sorption and scanning electron microscopy. We established the reasons behind the occurrence of such large porosity (>90%) in these films -- the replacement of reactive surface silanol groups with unreactive trimethylsilyl groups prevented the gel from forming further bridging bonds when being compacted under capillary stress. This resulted in a dilation or "springback" of the film once the stress was relaxed by nearly complete evaporation of the pore liquid (elastic response). In contrast, the films that were not surface-modified formed bonds under compaction so that they remained in the deformed state even when the capillary stress was released, resulting in low porosity (viscous response). This paper is an extension of the previous work and is based upon the visual observation of "springback" using ESEM and a quantitative comparison of aerogel, xerogel and pure solvent profiles from imaging ellipsometry. Stress measurements on the aerogel film using a cantilever-beam technique are also presented.

EXPERIMENTAL

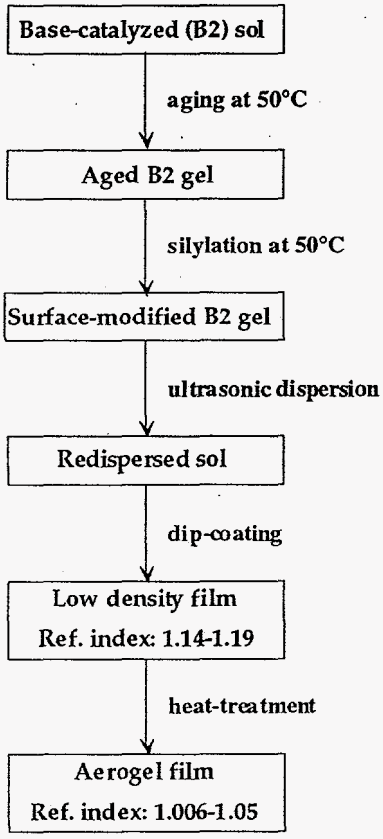

Figure 1. Schematic for the ambient-pressure aerogel film process.

Preparation of aerogel films

Silica films with refractive indices in the range of 1.006-1.05 (equivalent volume porosity 98.5-88%) were prepared at ambient pressure by an optimized process wherein organo-siloxane polymers are deposited onto a silicon substrate by conventional dip-coating at room temperature and heating to 450°C. A schematic illustrating the preparation of these films is shown in Figure 1. A detailed description of the process could be found in references 1 & 2. The film thicknesses (from SEM) vary from 0.1-3.5 μm, depending upon the dip-coating rate (0.5-19 mm/s) and concentration of the sol.

In-situ characterization by ellipsometric imaging

In order to observe the evolution of film porosity, the film deposition process was studied *in situ* using a home-made broad-beam ellipsometric imaging setup shown schematically in Figure 2. Aerogel, xerogel and pure solvent (ethanol) films were studied. The sols were ethanol-based. The xerogel film was made by the same process as shown in Figure 1 only excluding the surface-modification step. Refractive index and film thickness profiles of an ~1cm region around the drying line were obtained. The experimental setup and the theory involved behind the determination of the profiles are described in detail elsewhere[1,8].

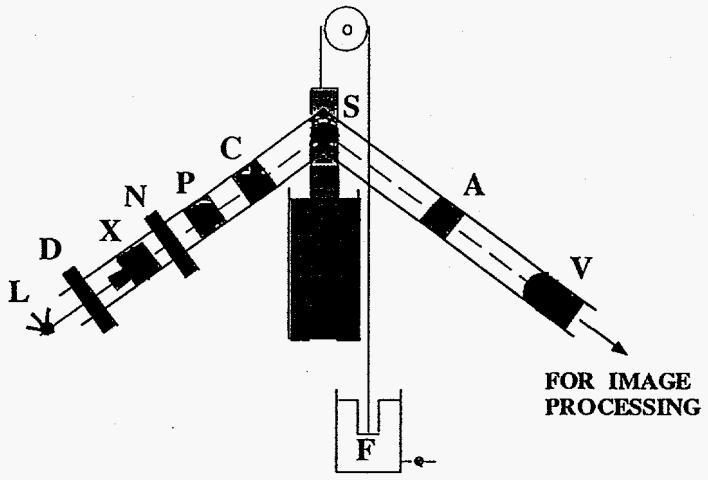

Figure 2. Schematic of imaging ellipsometry apparatus used to study film deposition in situ. L - monochromatic light source, D - polarizer, X - beam expander, N - diffuser, P - polarizer, C - compensator, A - analyzer, V - video camera, F - float.

To understand the deformation of these films in the presence of liquid-vapor menisci, the films were studied under the ESEM (Electroscan). Thick, crack-free aerogel films (~3.5 μm) were used. The dry sample, mounted on a stage, was placed in the ESEM chamber operating at a constant pressure of 5 Torr. The maximum operating pressure limit on the ESEM is ~10 Torr. The temperature of the stage (and hence, the sample) was controlled between -10 and +40°C by circulating 54% aqueous ethylene glycol solution from an external chiller. The chamber was filled with pure n-butanol vapor. Vapor condensation onto and liquid re-evaporation from the film were controlled by varying the temperature. The thickness of the film was monitored at different temperatures, allowing observation of its dependence on capillary pressure. The process was continuously recorded onto a video tape. In a different experiment, water vapor was allowed to condense onto the film to observe its wetting behavior.

RESULTS AND DISCUSSION

The ESEM experiments proved the reversibility of aerogel film deformation beyond doubt. Starting from a value of ~3.5 μm (dry film thickness), the film shrank as it was cooled to below 15°C at a constant pressure of 5 Torr (cooling cycle). This was consistent with the fact that more solvent (n-butanol) was entering the pores and capillary pressure was being developed. Between +4 and -3°C, the thickness reached its minimum of ~0.53 μm. As the temperature was lowered below -3°C, the film exhibited swelling and below -9°C expanded to near dry film thickness. It is easy to understand that this swelling is caused due to the flattening of the liquid-vapor meniscus as more solvent enters the pores, consequently lowering capillary pressure. On retracing the temperature path (heating cycle), the film shrank steadily, reached minimum thickness around 0°C and at ~3°C exhibited a sudden "springback" from ~1.7 to 3.5 μm. Thus, the deformation was almost perfectly reversible. The maximum deformation with respect to the minimum film thickness was ~500%! Snapshots at various stages of deformation are shown in Figure 3. In a different experiment, the non-wetting behavior of water with the film surface was observed (hydrophobicity).

Refractive index and thickness profiles were obtained from *in situ* ellipsometric imaging of the films during deposition. Figure 4 shows the aerogel thickness profile in an ~1cm region around the drying line. The coating rate used was 0.939 mm/s. The zero on the X-axis is a fixed point with respect to the steady-state film (and hence, to the lab frame). A smooth curve fit is applied to the data. The "springback" zone is magnified in Figure 4b. The data indicate rapid shrinkage upto the drying line and a thickness increase of ~100% upon "springback".

Figure 5 shows thickness profile data near the drying line for the xerogel and pure solvent (ethanol) films. Parabolic curve fits are applied to the data. The dip-coating speeds used were

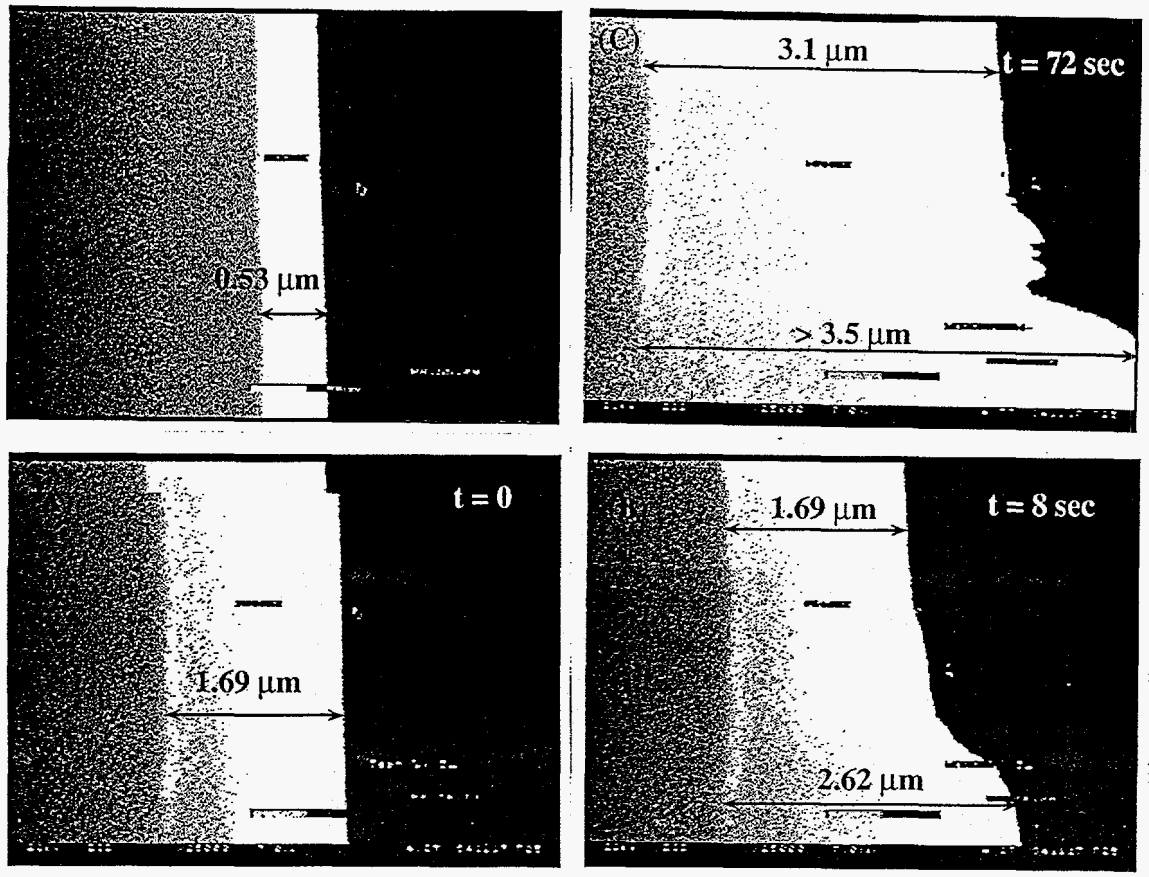

Figure 3. Snapshots of aerogel film deformation from ESEM. Counter-clockwise from top left - film at maximum state of compaction, A→C dynamic "springback" with release of capillary stress in the pores upon complete evaporation of the solvent.

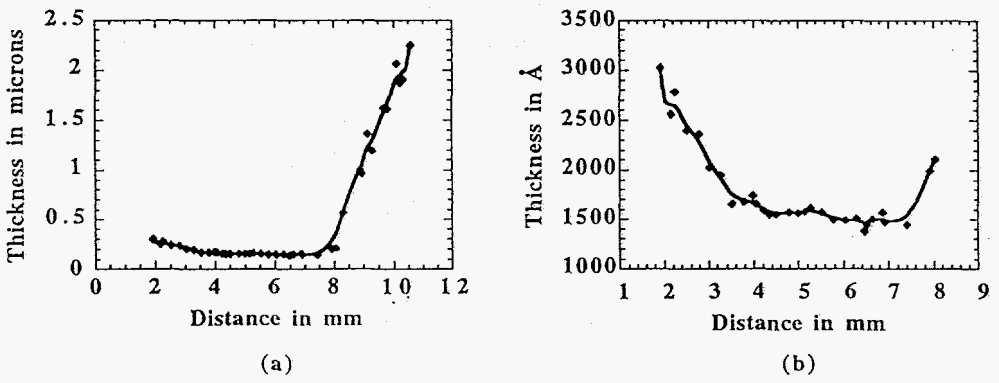

Figure 4. (a) Thickness profile of aerogel film, (b) Magnified view of thickness profile of aerogel film in "springback" zone.

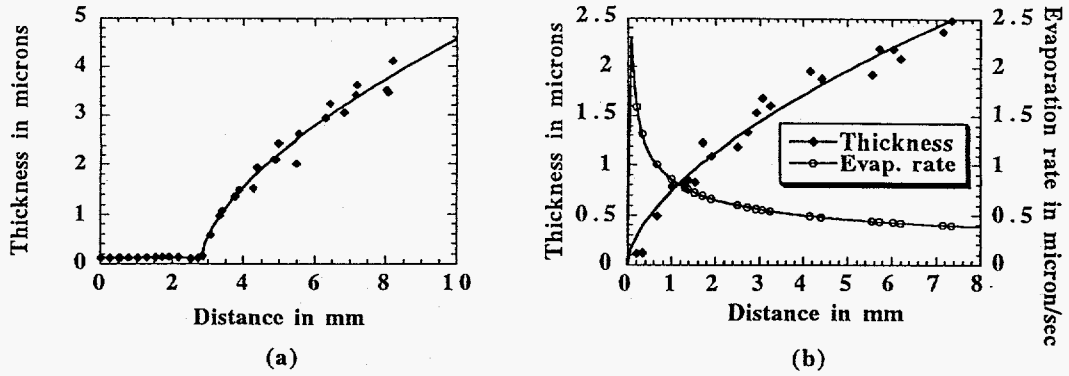

Figure 5. (a) Thickness profile of xerogel film, (b) Thickness and evaporation rate profiles of pure ethanol film.

1.08 mm/s for the xerogel film and 1.898 mm/s for the ethanol film. The equations for the fits are ("y" denotes thickness in μm and "x" the distance in mm relative to an arbitrary point fixed with respect to the steady-state film):

Xerogel: $y = 0.1220 + 0.01515\,x$ for $0 \le x \le 2.8375$ (1)

$y = 0.1650 + 1.254\,(x - 2.8375)^{0.638}$ for $x \ge 2.8375$ (2)

Ethanol: $y = 0.7372\,x^{0.610}$ (3)

Evaporation rate (μm/s) $= Y = -\frac{dy}{dt} = 0.8522\,x^{-0.390}$ (4)

For the xerogel film, the thickness at x = 0 is 1220 Å and refractive index (n) 1.2829. This was in excellent agreement with the corresponding values measured with a commercial ellipsometer (Gaertner Scientific Corporation Model L116C) -- 968 Å and 1.275. The thickness difference indicates that shrinkage does not stop at the drying line, but continues at a much slower rate till the steady, dry film thickness is reached. For the ethanol film, the majority of the calculated Ψ, Δ values fell within the n = 1.30 and 1.40 trajectories (literature value: $n_{ethanol} = 1.36$).

Stress measurements done by Samuel[9] using the cantilever-beam method showed that mechanical stresses in the ambient-pressure aerogel films were at least an order of magnitude lower than those seen in typical acid-catalyzed (A2) sol-gel films. The maximum macroscopic stress (different from the solid network and capillary stresses) that causes deflection of the substrate was measured to be ~4 Kbar for the A2 film and ~0.15 Kbar for the aerogel film.

The ambient-pressure aerogel films exhibit a variety of extraordinary features, the most striking of which are its reversible deformation with capillary stress, its hydrophobicity and its higher critical cracking thickness. In our earlier work[1], we underlined the role played by surface hydroxyl groups in determining the reversibility during deformation. Our observation of near 100% reversibility using ESEM is consistent with the FTIR spectroscopic observations[1] that

there are no hydroxyls present in the dry aerogel film at <150°C. It must however be emphasized, that the sol used to prepare the aerogel films contained a definite number of hydroxyls, which enabled the formation of a continuous gel-network. This explained the film-cracking that was observed at high concentrations of the silylating group. The profiles quantified the contrasting behavior of the xerogel (irreversible deformation) and aerogel films. Thus, during the final stage of drying (pore emptying stage) one can safely conclude that the aerogels exhibit elastic behavior (strain $\propto$ stress), while the xerogels exhibit viscous behavior (strain rate $\propto$ stress). Another important feature of the aerogel films is their hydrophobicity. Typical sol-gel films (xerogels) due to the presence of residual surface hydroxyls adsorb water from the atmosphere, causing them to be in a permanent state of stress. The hydrophobicity of the aerogel films imparts greater stability and larger thicknesses to these films. Finally, the preparation of thick aerogel films (~3.5 μm) was consistent with the stress measurements, indicating that they have a higher critical cracking thickness than the typical value of ~ 1 μm.

CONCLUSIONS

This study firmly established the reversibility of ambient-pressure aerogel film deformation. The reason behind the appearance of high porosity is explained in comparison with xerogel films. Also, the observation of higher film thicknesses is better understood, now.

ACKNOWLEDGMENTS

The authors thank Sudeep Rao and Donald Stuart for their assistance with the ESEM and imaging ellipsometry setup respectively and Joshua Samuel for the stress measurements.

REFERENCES

1. S.S. Prakash, C.J. Brinker and A.J. Hurd, International Symposium of Aerogels-4 Proceedings to be published in special issue of Journal of Non-Crystalline Solids, 1994.
2. C.J. Brinker and S.S. Prakash, U.S. Patent Application, 1994.
3. L.W. Hrubesh and J.F. Poco, International Symposium of Aerogels-4 Proceedings to be published in special issue of Journal of Non-Crystalline Solids, 1994.
4. S.S. Kistler, *Nature*, 127, p 741, (1931).
5. C.J. Brinker and G.W. Scherer, "Sol-Gel Science: The Physics and Chemistry of Sol-Gel Processing", Academic Press, San Diego, CA (1990).
6. D.M. Smith, R. Deshpande and C.J. Brinker, "Better Ceramics Through Chemistry V", Eds. M.J. Hampden-Smith, W.G. Klemperer and C.J. Brinker, Mat. Res. Soc. Symp. Proc., Vol. 271, Pittsburgh, PA (1992), p 567-572.
7. D.J. Stein, A. Maskara, S. Hærid, J. Anderson and D.M. Smith, "Better Ceramics Through Chemistry VI", Eds. A.K. Cheetham, C.J. Brinker, M.L. Mecartney and C. Sanchez, Mat. Res. Soc. Symp. Proc., Vol. 346, Pittsburgh, PA (1994), p 643-648.
8. A.J. Hurd and C.J. Brinker, "Better Ceramics Through Chemistry III", Eds. C.J. Brinker, D.E. Clark and D.R. Ulrich, Mat. Res. Soc. Symp. Proc., Vol. 121, Pittsburgh, PA (1988), p 731-742.
9. J. Samuel, private communication.

***This work was supported by the DOE on contract number DE-AC04-94AL85000 at Sandia National Laboratories.